International Journal of Heat and Fluid Flow 49 (2014) 11–17

Contents lists available at ScienceDirect

International Journal of Heat and Fluid Flow

journal homepage: www.elsevier.com/locate/ijhff

New results on the structure of turbulence in a mixing layer with and without swirl

Samuel Davoust, Laurent Jacquin *, Benjamin Leclaire

Department of Fundamental and Experimental Aerodynamics, ONERA, The French Aerospace Lab, F-92190 Meudon, France

ARTICLE INFO

Article history:
Available online 12 July 2014

Keywords:
Mixing layer
Mixing layer turbulence
Swirl
High-speed piv

ABSTRACT

The near field of a 2.14×10^5 Reynolds number, low-Mach-number, cylindrical jet with and without swirl has been investigated by high-speed stereo PIV in a transverse plane, two diameters downstream of the jet exit. Using spatiotemporal correlations, we investigate the dynamics of streamwise vorticity in the shear layer, responsible for the mixing properties of the jet, and show how swirl affects this vorticity. A dynamical scenario is proposed, which explains how the mean shear and the azimuthal $m = 0$ vortices contribute to the spatial organization observed.

1. Introduction

Organization of turbulence in a jet flow has remained an active field of research since early studies, due to the needs of accurate predictions in the fields of mixing, combustion and acoustics. In these applications, jets also often exhibit a degree of swirl, which may have a significant impact on this mixing. In past studies, the description, modeling and control of the large-scale structures in these jets have been recognized as major objectives. In the near field, the main dynamical features are known to be $m = 0$ and $m = 1$ oscillations of the jet column, m denoting the Fourier azimuthal wavenumber, along with streamwise vortical structures in the mixing layer and smaller-scale turbulence. Despite a large number of studies, the mechanism creating these vortices remains not fully determined, and also seems to be dependent to the Reynolds number and initial conditions. A detail physical understanding of the ability of swirl to enhance mixing also seems to be lacking. Our aim in this communication is to refine these views, in the case of a 2.14×10^5 Reynolds number, low-Mach-number, cylindrical jet, which may or not exhibit a large central zone of solid-body rotation. We measure the jet near field velocity by stereo PIV in longitudinal planes, and in a transverse plane located at two diameters from the exit. In this plane, the acquisition is performed at high frequency. We use these measurements to first characterize the evolution with swirl of the global mixing layer properties (spreading rate, maximum turbulent kinetic energy), and then to investigate in detail the dynamics of the coherent structures involved in the mixing process. We focus here in particular on the streamwise vortices, and their interaction with the $m = 0$ modes. Finally, we propose dynamical scenarios which account for the origin and spatial structures of these vortices.

2. Experimental setup

2.1. Control parameters

We use an open return wind tunnel, which has been designed originally to study the effect of rotation on turbulence (Jacquin et al., 1990). In this facility, a centrifugal blower first drives the flow into a diffuser followed by a settling chamber. The flow then undergoes a first contraction from a 1 m square cross-section to a circular $D_c = 300$ mm cross-section. As sketched in Fig. 1, a 500 mm long part of this cylindrical duct can be put into rotation with a controlled angular velocity Ω_c that can reach $1000_{\text{r.p.m}}$. The rotating part contains a 100 mm long honeycomb with 1.5 mm cell diameter. The jet, of exit diameter $D_0 = 150$ mm, is then generated by a contracting nozzle (contraction ratio $\chi = 4$, $L_c/D_c = 1.26$), ended by a 150 mm long thin edged nozzle. As the contraction tends to relaminarize the upstream turbulent boundary layer, the boundary layer in the nozzle is tripped 48 mm upstream of the exit section with a carborandum strip composed of particles of 0.25 mm nominal diameter. The exit bulk velocity U_0 is defined by

$$U_0 = \frac{\dot{m}_0}{\rho \pi D_0^2/4} = \frac{\int_0^{0.5} u_z(z=0,r) r dr}{\int_0^{0.5} r dr} \qquad (1)$$

where the exit flow rate m_0 is kept constant thanks to a Venturi flow meter placed upstream of the fan air intake. The corresponding Reynolds number is

* Corresponding author. Tel.: +33 146235153.
E-mail address: laurent.jacquin@onera.fr (L. Jacquin).

http://dx.doi.org/10.1016/j.ijheatfluidflow.2014.05.012
0142-727X/

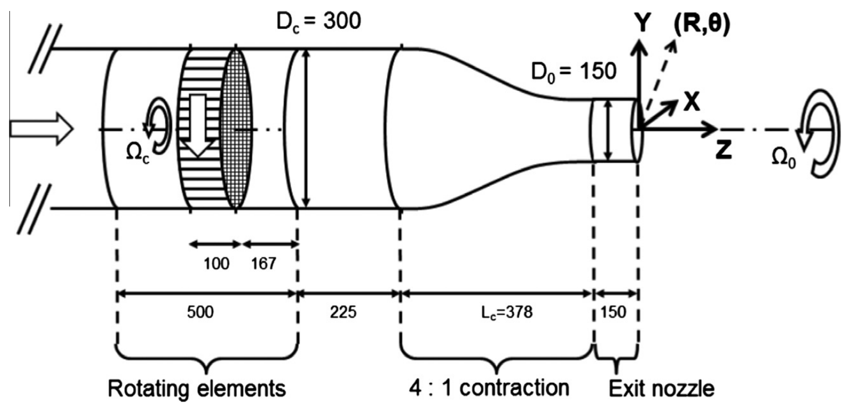

Fig. 1. Principle sketch of the swirling jet generation and frame of references. Dimensions are given in mm.

$$\mathrm{Re}_0 = \frac{U_0 D_0}{\nu} = 2.14 \times 10^5 \quad (2)$$

As far as rotation effects are concerned, the control parameter is the jet swirl number:

$$S_0 = \frac{\Omega_0 D_0/2}{U_0} \quad (3)$$

where Ω_0 is the angular velocity of the exit flow. After contraction one has $\Omega_0 \approx \chi\Omega_c$ so that imposing the rotation rate Ω_c of the honeycomb amounts to control the flow conditions by means of the control swirl number:

$$S = \frac{\chi\Omega_c D_0/2}{U_0} \quad (4)$$

The same definition was used by Liang and Maxworthy (2005). As shown by Leclaire and Jacquin (2012), the exit flow is in solid body rotation except for the boundary layers, and with a low axial turbulence level in the core (0.5%), up to $S = 0.81$. This fixes the maximal swirl value considered in the present study.

2.2. Measurements

We perform several Stereo PIV (SPIV) acquisition in different planes, as shown in Fig. 2. Longitudinal planes, labeled M1–M5 and J1–J4, correspond to a low frame rate, 4 Hz acquisition of $N = 5000$ samples per run. The $z = 2$ cross-sectional plane is investigated with High Speed SPIV (HS-SPIV). In this plane, 30 blocks of 2048 samples are acquired at 2.5 kHz for each measurement point. Calibration of the cameras relies on a pin-hole model, and is followed by a self-calibration as in Wieneke (2005), in order to correct any misalignment between the calibration plate and the laser sheet.

Vector computation is performed using the ONERA in-house software FOLKI-SPIV, which is implemented on GPU (Champagnat et al., 2011) and uses a novel paradigm for Stereo PIV (Leclaire et al., 2012). In all cases, an interrogation window of 31 × 31 pixels is chosen for image interrogation, corresponding to a variable spatial resolution depending on the PIV plane. Results are sampled every 13 pixels in the M1–M5 and J1–J4 planes (60% overlap), and every 30 pixels in the HS-SPIV plane. In the latter case, this choice stems from the large amount of data involved. An uncertainty analysis shows that no significant peak-locking is present, and leads to an overall uncertainty of 0.3 m.s^{-1}, that is, 1.5% of U_0. Further details, as well as the effect of spatial filtering especially in the HS-SPIV plane, can be found in Davoust et al. 2012, and Davoust, 2012. In these studies, the sampling and post-processing were carefully validated against hot-wire measurements. The hot wire technique was also used to characterise the boundary layer in the exit plane of the nozzle.

3. Jet axial development

In all the following, dimensionless quantities will be considered, with the exit bulk velocity U_0 and the jet exit diameter D_0 respectively taken as velocity and length references.

We first account for the evolution of the mean flow axial development with respect to S, which is illustrated in Fig. 3. Here, mean axial and azimuthal velocity profiles are represented in a longitudinal planes, at selected values of the axial coordinate z, and the turbulent kinetic energy k is represented with grey levels.

From $S = 0$ to $S = 0.81$, apart from the appearance and the gradual increase of the azimuthal velocity, one can observe several changes, which are pronounced mostly for $S = 0.61$ and $S = 0.81$. First, the length of the potential core decreases. This is associated to a higher spatial growth rate and higher turbulent kinetic energy

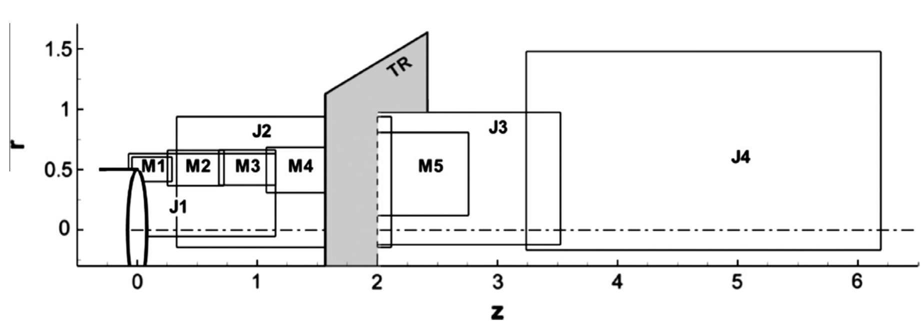

Fig. 2. Location of the stereo PIV measurement planes performed. White planes identify low frame rate SPIV, and the gray plane high speed SPIV. The axial and radial coordinates are normalized with the jet exit diameter D_0.